# Novel grating design approach by radiation modes coupling in nonlinear optical waveguides

**A. Massaro[*], R. Cingolani[*], M. De Vittorio[*], and A. Passaseo[*A]**

*[*] National Nanotechnology Laboratory of CNR-INFM , Distretto Tecnologico-ISUFI, Università del Salento, Via Arnesano 16, 73100 Lecce, Italy.*

*[A] Permanent address: IMM CNR sezione Lecce, University Campus, Lecce-Monteroni 73100, Italy*

*alessandro.massaro@unile.it*

**Abstract:** In integrated optics the radiation modes represent a negative aspect regarding the propagation of guided modes. They characterize the losses of the substrate region but can contribute to enhance the guided modes by considering the coupling through properly designed gratings arranged at the core/substrate interface. By tailored gratings, the radiation modes become propagating modes and increase the guided power inside the waveguide guiding region. This enhancement is useful especially in low intensity processes such as second harmonic $\chi^{(2)}$ conversion process. For this purpose, we analyze accurately the radiation modes contribution in a $\chi^{(2)}$ GaAs/AlGaAs nonlinear waveguide where second harmonic signal is characterized by a low power intensity. This analysis considers a new design approach of multiple grating which enhances a fundamental guided mode at $\lambda_{FU}$ =1.55 μm and a codirectional second harmonic guided mode at $\lambda_{SH}$ =0.775 μm. In particular we analyze the second harmonic conversion efficiency by studying the coupling effect of three gratings. The combined effects of the gratings provide an efficient second harmonic field conversion. Design considerations, based on the coupled mode equations analysis, are theoretically discussed. A good agreement between analytical and numerical results is observed.



**OCIS codes:** (000.4430) Numerical approximation and analysis; (310.0310) Thin films.

## References and links

1. E. U. Rafailov, P. L. Alvarez, C. T. A. Brown, W. Sibbett, R. M. De la Rue, P. Millar , D. A. Yanson, J. S. Roberts, and P. A. Houston, "Second-harmonic generation from a first-order quasi-phase-matched GaAs/AlGaAs waveguide crystal," Opt. Lett. **26**, 1984-1986 (2001). .
2. X. Yu, L. Scaccabarozzi, J. S. Harris, P. S. Kuo, and M. M. Fejer, "Efficient continuous wave second harmonic generation pumped at 1.55 μm in quasi-phase-matched AlGaAs waveguides," Opt. Express **13**, 10742-10748 (2005).
3. X. Yu, L. Scaccabarozzi, A. C. Lin, M. M. Fejer, and J. S. Harris, "Growth of GaAs with orientation-patterned structures for nonlinear optics," J. Cryst. Growth **301**, 163-167 (2007).
4. A. Massaro, V. Tasco, M. T. Todaro, R. Cingolani, M. De Vittorio, and A. Passaseo, "Scalar time domain modeling and coupling of second harmonic generation process in GaAs discontinuous optical waveguide," Opt. Express **16**, 14496-14511 (2008).
5. T. Rozzi and M. Mongiardo, *Open Electromagnetic Waveguides*, (IEE Electromagnetic Waves Series 43, London 1997).
6. D. Marcuse , *Theory of Dielectric Optical Waveguides* (Academic Press, New York 1974).
7. D. Marcuse, "Hollow dielectric waveguides for distributed feedback lasers," IEEE J. Quantum Electron. **26**, 1265-1276 (1972).
8. T. Suhara, and M. Fujimura, *Waveguide Nonlinear-Optic Devices* (Berlin: Springer, 2003).
9. T. Suhara, and H. Nishihara, "Theoretical analysis of waveguide second-harmonic generation phase matched with uniform and chirped grating," IEEE J. Quantum Electron. **8**, 661-669 (1972).
10. S. Ura, S. Murata, Y. Awtsuji, and K. Kintaka, "Design of resonance grating coupler," Opt. Express **16**, 12207-12213 (2008).
11. A. Massaro, and T. Rozzi, "Rigorous time-domain analysis of dielectric optical waveguides using Hertzian potentials formulation," Opt. Express **14**, 2027-2036 (2006).

#106111 - $15.00 USD Received 7 Jan 2009; revised 24 Feb 2009; accepted 9 Mar 2009; published 13 Apr 2009

12. A. Taflove, S. C. Hagness, *Computational Electrodynamic: the Finite-difference Time-domain Method,* (Arthec House Publishers, sec. ed., London 2000), ch. 2,3,4,7.
13. G. Mur, "Absorbing boundary conditions for the finite-difference approximation of the time-domain electromagnetic field equations," IEEE Trans. Electromagn. Compat. **23**, 377-382 (1981).

## 1. Introduction

Studies of $\chi^{(2)}$ and the quasi-phase matching (QPM) technique promote research works on nonlinear optic (NLO) devices for ultrafast signal processing based on second-order nonlinearity. After the development of high-efficiency QPM- second harmonic generation (SHG) devices using ferroelectric crystal waveguides, the research was directed to implementation of a compact and efficient coherent light source by combining the SHG device with a semiconductor laser. Moreover a strong motivation of research on NLO devices has been the need for the development of all-optical wavelength converters for dense wavelength division multiplexing (DWDM) optical communication systems. In particular the second harmonic generation in $\chi^{(2)}$ nonlinear process represents a good solution for DWDM applications in telecommunication systems. But this process requires high intensity input power and large interaction lengths for a good second harmonic (SH) conversion. For this reasons the introduction of tailored gratings which enhance the SH field is important.

The novel design approach proposed in this work takes into account the multiple grating effects which enhance the guided SH signal along the symmetrical waveguide shown in Fig. 1. The new accurate analysis concerns the coupling of the radiation modes with the propagating fundamental and SH modes: properly designed gratings, arranged at the core/substrate interface, generate scattered waves which increase the guided modal power inside the waveguide guiding region. By tailored gratings, the radiation modes supply energy to the low intensity SH mode by providing an efficient SH conversion in short structures. In the presented structure three grating are considered: the first grating (grating 1 of Fig. 1), considered at one interface between core and substrate, is designed by quasi phase matching QPM condition. The QPM technique is a practical method of substantially increasing the second-harmonic power by effectively reducing the phase mismatch between the fundamental and the SH fields: the technique relies on introducing the grating 1 in the waveguide to compensate for the difference of the propagation refractive indexes in the waveguide.

A second grating (grating 2 of Fig. 1), placed at second the interface between the core and the substrate region, increases the fundamental power through the coupling between the substrate modes and the fundamental guided mode. On the same second interface, after the grating 2, we consider a third grating (grating 3 of Fig. 1) which enhances the power transferred to the SH mode through the coupling between the substrate modes and the SH guided mode by optimizing the conversion efficiency.

The substrate modes are excited through the diffraction effect of the grating 2 and 3 of Fig. 1 which supply the energy to both the propagating fields through the coupled energy of the radiation modes. The coupling effect is analyzed by combining the coupled mode equations systems related to the three grating. The novelty of this work is in the combined effect of the three gratings applied to a symmetrical GaAs/AlGaAs waveguide typically used in NLO devices [1]-[3]. In particular we analyze the enhancement of a SH signal ($\lambda_{SH}$= 0.775 μm) generated by a codirectional fundamental mode ($\lambda_{FU}$= 1.55 μm). The goal of the presented work is to find the optimum geometrical configuration which overcomes the problems associated to the total waveguide length such as reflections and losses, by providing a good SH field conversion. With the introduction of the multiple grating configuration it is possible to decrease the total waveguide length by obtaining a good conversion efficiency according to real input powers.

We resume the analysis of this work in the following steps: i) we analyze the modes involved in the designed structure including substrate modes and diffraction theory; ii) we study the coupled mode equations systems by combining the effect of each grating; iii) we provide the design criteria steps of the periodic structure; iv) finally we model the tailored

#106111 - $15.00 USD Received 7 Jan 2009; revised 24 Feb 2009; accepted 9 Mar 2009; published 13 Apr 2009

waveguide through the time domain Hertzian potential formulation (HPF) used to solve nonlinear $\chi^{(2)}$ processes [4], and by the finite difference time domain (FDTD) modelling. A good agreement between numerical and analytical results is checked.

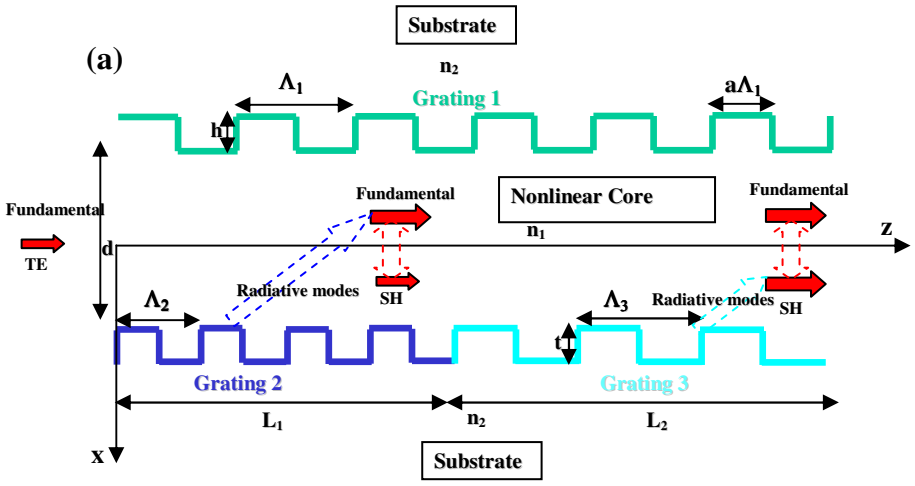


Fig. 1. Multiple gratings design in nonlinear optical symmetrical waveguide.

## 2. Modes of the discontinuous periodic waveguide.

As shown in Fig. 2, the symmetrical waveguide is characterized by a discrete set of orthogonal guided modes and by radiation modes. The radiation field (related to the radiation modes) thus qualifies in all aspects as a mode, except that is not confined to the waveguide core but reaches undiminished to infinite distance in $x$ direction normal to the core. The modes of this type are called radiation modes. Their propagation constant $\beta$ are not constrained to a discrete set of values, since they are related to the angle of the incident can be chosen arbitrarily. The values of the propagation constant thus form a continuum, so that we also speak of the radiation modes as modes of the continuum. The guided and radiation modes form a complete orthogonal set of modes. Any field distribution can be expressed by series expansion into these modes. All the modes are classified as transverse electric (TE) and as transverse magnetic (TM) modes. According to the assumption of TE polarized source, we limit the discussion to TE waves.

For the transverse electric (TE) field with no variation along the $y$-direction, only three field components exists, and they are related as follows

$$H_x(x,z) = \frac{1}{j\omega\mu}\frac{\partial}{\partial z}E_y(x,z)$$
$$H_z(x,z) = \frac{1}{j\omega\mu}\frac{\partial}{\partial x}E_y(x,z) \tag{1}$$

where $E_y$(x,z) may be expressed as a modal expansion [5]

$$E_y(x,z) = \left\{\sum_k a_k\psi_k(x) + \int_0^\infty b(k_x)\varphi(x;k_x)dk_x\right\}e^{-j\beta z} \tag{2}$$

#106111 - $15.00 USD Received 7 Jan 2009; revised 24 Feb 2009; accepted 9 Mar 2009; published 13 Apr 2009

and $a_k$ and $b(k_x)$ are the amplitudes of the guided and continuum modes respectively. In the case of two TE guided modes (fundamental and SH modes) the guided field are represented by [5]

$$E_y^{\omega} = a^{\omega}\psi^{\omega}(x)e^{-j\beta^{\omega}z}$$
$$E_y^{2\omega} = a^{2\omega}\psi^{2\omega}(x)e^{-j\beta^{2\omega}z} \tag{3}$$

with

$$\psi^{\omega,2\omega}(x) = \begin{cases} \cos(\sigma^{\omega,2\omega}x) & core \\ \cos(\sigma^{\omega,2\omega}d/2)\exp[-\Delta^{\omega,2\omega}(x-d/2)] & substrate \end{cases} \tag{4}$$

and

$$a^{\omega,2\omega} = \sqrt{\frac{d}{1+\frac{1}{\Delta^{\omega,2\omega}}}} \tag{5}$$

where the parameters $\sigma^{\omega,2\omega}$ and $\Delta^{\omega,2\omega}$ are defined by the following equations

$$\Delta^{\omega,2\omega} = (n_2^2(k^{\omega,2\omega})^2 - (\beta^{\omega,2\omega})^2)^{1/2} \tag{6}$$
$$\sigma^{\omega,2\omega} = (n_1^2(k^{\omega,2\omega})^2 - (\beta^{\omega,2\omega})^2)^{1/2} \tag{7}$$

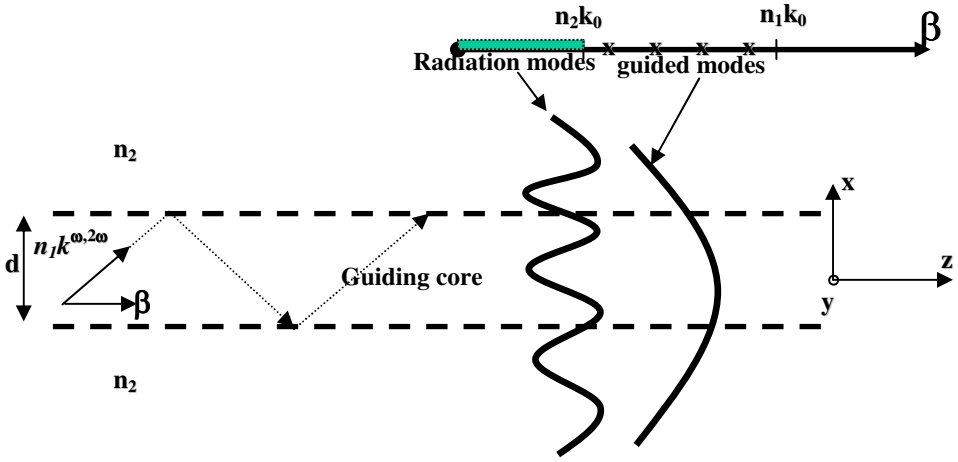


Fig. 2. Modes in symmetrical planar waveguide.

The radiation modes are necessary to describe radiation phenomena in region around the core. Imperfections, such as step discontinuities and sinusoidal core interface deformations, cause some of the guided mode power to radiate into the space outside and inside the core. The diffraction theory [6] of plane wave scattering from a sinusoidally deformed dielectric interface explains the radiation modes excitation mechanism. We assume that only two TE modes (fundamental and SH mode) are propagated inside the guiding core. The diffraction theory is applied at interface related to the grating 2 and 3 of Fig. 1. The theory is based on

#106111 - $15.00 USD Received 7 Jan 2009; revised 24 Feb 2009; accepted 9 Mar 2009; published 13 Apr 2009

approximate plane wave analysis [7] and on the sinusoidal approximation of one core-substrate interface [6],[7]. The function $f(z)$ which represents the sinusoidal interface deformation is given as

$$f(z) = t\sin\left(\frac{2\pi}{\Lambda_{2,3}}z\right) \tag{8}$$

As reported in Fig. 3 the sinusoidally deformed dielectric interface scatters the incident radiation. The arrows shown in the Fig. 3 indicate the propagation vector of the incident, reflected, and transmitted plane waves labeled i, r, and t. The shorter arrows labeled 1 and -1 indicate scattered plane waves. Two scattered waves emerge on either side of the interface. One set of scattered waves accompanies the reflected wave in the core region and another set accompanies the transmitted wave in the substrate region. The angle $\phi$ of the direction of each wave indicated in Fig. 3 is obtained from the equation

$$\cos(\phi) = \beta / n_i k^{\omega,2\omega} \tag{9}$$

where the propagation constant $\beta$ indicates either, $\beta^{\omega,2\omega}$, $\beta^{(+)}$, or $\beta^{(-)}$, $n_i$ stands for $n_1$ and $n_2$, and $k^{\omega,2\omega}= 2\pi/\lambda_{FU,SH}$. We observe that if the period $\Lambda_{2,3}$ satisfies the substrate mode condition

$$\left|\frac{2\pi}{\Lambda_{2,3}} \pm \beta^{\omega,2\omega}\right| < n_i k^{\omega,2\omega} \tag{10}$$

for $i$=1, and $i$=2, propagating scattered waves will exist. Far from the surface only the zero-order reflected and transmitted waves can be observed. Only in the immediate vicinity of the distorted surface is there any field distortion. Though the grating, this distorted field exchanges power with the zero-order field by increasing the guided power. The field of zero-order are the incident i, reflected r, and transmitted t plane waves corresponding to the fundamental and SH fields. In particular in the TE case the zero-order field is given by

$$e_y^{\omega,2\omega} = A_i \exp[-j(\sigma^{\omega,2\omega}x + \beta^{\omega,2\omega}z)] + A_r \exp[j(\sigma^{\omega,2\omega}x - \beta^{\omega,2\omega}z)] \quad \textit{core region} \tag{11}$$

$$e_y^{\omega,2\omega} = A_t \exp[-j(\Delta^{\omega,2\omega}x + \beta^{\omega,2\omega}z)] \qquad \text{substrate } \textit{region} \tag{12}$$

The total scattered field includes in each region the contributions of the scattered field $a^{+}_{\gamma i}$ and $a^{-}_{\gamma i}$ of Fig. 3 , and is represented by [7]

$$E_y^S = \frac{t}{2}A_i\sigma^{\omega,2\omega}(\Delta^{\omega,2\omega} - \sigma^{\omega,2\omega})\left[\frac{\exp[-j(\sigma^{(-)}x - \beta^{(-)}z)]}{\sigma^{(-)} + \Delta^{(-)}} - \frac{\exp[j(\sigma^{(+)}x - \beta^{(+)}z)]}{\sigma^{(+)} + \Delta^{(+)}}\right] \tag{13}$$

*core region*

$$E_y^S = \frac{t}{2}A_i\sigma^{\omega,2\omega}(\Delta^{\omega,2\omega} - \sigma^{\omega,2\omega})\left[\frac{\exp[-j(\Delta^{(-)}x + \beta^{(-)}z)]}{\sigma^{(-)} + \Delta^{(-)}} - \frac{\exp[-j(\Delta^{(+)}x + \beta^{(+)}z)]}{\sigma^{(+)} + \Delta^{(+)}}\right] \tag{14}$$

*substrate region*

with the definitions [7]

#106111 - $15.00 USD Received 7 Jan 2009; revised 24 Feb 2009; accepted 9 Mar 2009; published 13 Apr 2009

$$\beta^{(\pm)} = \beta^{\omega,2\omega} \pm \frac{2\pi}{\Lambda_{2,3}} \tag{15}$$

$$\sigma^{(\pm)} = (n_1^2 (k^{\omega,2\omega})^2 - (\beta^{(\pm)})^2)^{1/2} \tag{16}$$

$$\Delta^{(\pm)} = (n_2^2 (k^{\omega,2\omega})^2 - (\beta^{(\pm)})^2)^{1/2} \tag{17}$$

where (15) indicates the phase matching between the zero order field and the scattered waves.

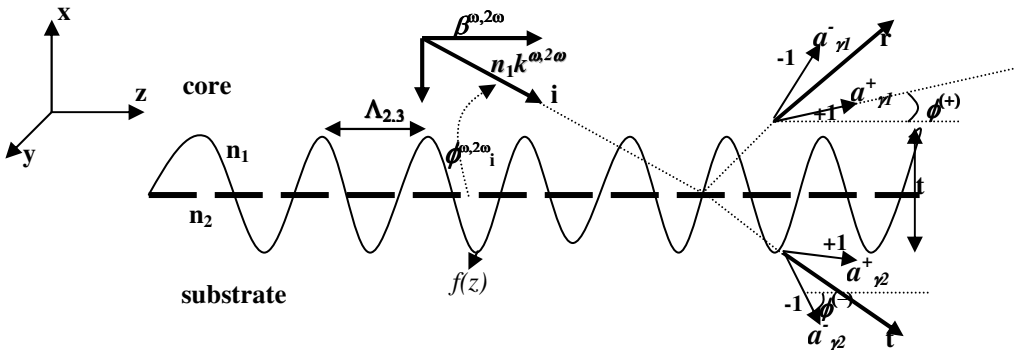


Fig. 3. The sinusoidally distorted core-substrate interface acts like a phase grating. The incident i, reflected r, and diffracted rays are shown. The sinusoidal approximation is applied to the grating 2 and 3 of Fig. 1.

### 3. Coupled mode theory.

In our analysis three coupled equations system are considered. The first set of coupled equations is related to grating 1 of Fig. 1. The function of this grating is to couple the fundamental field with the SH field. In particular by indicating with $A^{\omega}$ the amplitude of the pump fundamental field and with $A^{2\omega}$ the amplitude of the SH wave we obtain [8],[9]

$$\begin{cases} \dfrac{dA^{\omega}(z)}{dz} + j(2k_L^{\omega}\cos Kz)A^{\omega}(z) \\ \qquad\qquad = -\,j[k_{NL}\exp(j2\delta z)]^*[A^{\omega}(z)]^* A^{2\omega}(z) \\ \dfrac{dA^{2\omega}(z)}{dz} + j(2k_L^{2\omega}\cos Kz)A^{\omega}(z) \\ \qquad\qquad = -\,jk_{NL}\exp(j2\delta z)[A^{\omega}(z)]^2 \end{cases} \tag{18}$$

with

$$k_L^{\omega} = \frac{\omega\varepsilon_0}{4}\int [E_y^{\omega}(x)]^* \Delta\varepsilon E_y^{\omega}(x)dx \tag{19}$$

$$k_L^{2\omega} = \frac{2\omega\varepsilon_0}{4}\int [E_y^{2\omega}(x)]^* \Delta\varepsilon E_y^{2\omega}(x)dx \tag{20}$$

#106111 - $15.00 USD Received 7 Jan 2009; revised 24 Feb 2009; accepted 9 Mar 2009; published 13 Apr 2009

$$k_{NL} = \frac{2\omega\varepsilon_0}{4}\int [E_y^{2\omega}(x)]^* \tilde{\chi}_{NL}[E_y^{\omega}(x)]^2 dx \tag{21}$$

where

$$2\delta = \beta^{2\omega} - (2\beta^{\omega} + K), \quad K = 2\pi/\Lambda_1 \tag{22}$$

is the phase mismatch between the fundamental and SH field ,

$$\Delta\varepsilon = (\varepsilon_1 - \varepsilon_2)\frac{\sin(a\pi)}{\pi}\exp[-jKz] \tag{23}$$

is the first term of the permittivity Fourier series, and finally

$$\tilde{\chi}_{NL} = (\chi_1^{(2)} - \chi_2^{(2)})\frac{\sin(a\pi)}{\pi}\exp[-jKz] \tag{24}$$

is the first term of the nonlinear coefficient Fourier series, and *a* denotes the duty ratio of the period.

The grating 2 of Fig. 1 enhances the low pump fundamental field coupled into the waveguide. In this case coupling between the fundamental field and the scattered fields (generated by grating 2) is considered. In particular the equations to solve are the following [10]

$$\begin{cases} \dfrac{dA^{\omega}(z)}{dz} = -j\sum_i \int a_{\gamma i}^{\pm}(z) k^*_{\gamma i, A^{\omega}} \exp[-j(\beta^{\pm} - (\beta^{\omega} - 2\pi/\Lambda_2)z]d\beta^{\pm} \\ \dfrac{da_{\gamma i}^{\pm}(z)}{dz} = -jA^{\omega}(z) k^*_{\gamma i, A^{\omega}} \exp[-j(\beta^{\pm} - (\beta^{\omega} - 2\pi/\Lambda_2)z] \end{cases} \tag{25}$$

with the coupling coefficient defined as

$$k_{\gamma i, A^{\omega}} = k_S^{\omega} = \int E_y^{\omega}(x)\Delta\varepsilon E_y^S(x)dx \tag{26}$$

Finally the grating 3 optimize the SH conversion by coupling the SH field with the scattered field. In particular we take into account the system

$$\begin{cases} \dfrac{dA^{2\omega}(z)}{dz} = -j\sum_i \int a_{\gamma i}^{\pm}(z) k^*_{\gamma i, A^{2\omega}} \exp[-j(\beta^{\pm} - (\beta^{\omega} - 2\pi/\Lambda_3)z]d\beta^{\pm} \\ \dfrac{da_{\gamma i}^{\pm}(z)}{dz} = -jA^{2\omega}(z) k^*_{\gamma i, A^{2\omega}} \exp[-j(\beta^{\pm} - (\beta^{\omega} - 2\pi/\Lambda_3)z] \end{cases} \tag{27}$$

where

$$k_{\gamma i, A^{2\omega}} = k_S^{2\omega} = \int E_y^{2\omega}(x)\Delta\varepsilon E_y^S(x)dx \tag{28}$$

#106111 - $15.00 USD Received 7 Jan 2009; revised 24 Feb 2009; accepted 9 Mar 2009; published 13 Apr 2009

## 4. Design and results

We assume that the fundamental pump source ($\lambda_{FU}$=1.55 μm) is a polarized TE field. The GaAs core ($n_1(\lambda_{FU}$=1.55 μm)=3.374 and $n_1(\lambda_{SH}$=0.755 μm)=3.691) is characterized by a thickness d=0.22 μm and supports only a TE fundamental mode at $\lambda_{FU}$=1.55 μm and only a SH TE mode at $\lambda_{FU}$=0.775 μm. In this way all the TE power is matched with the two propagating modes and the modal dispersion is low. In order to minimize the reflections along the *z*- propagating the direction and to conserve the single mode condition, the parameters h and t of Fig. 1 are fixed to the low value of 0.025 μm. The substrate material is $Al_{0.4}Ga_{0.6}As$ ($n_2(\lambda_{FU}$=1.55 μm)=3.2 and $n_2(\lambda_{SH}$=0.755 μm)=3.4). The GaAs core, combined with the $Al_{0.4}Ga_{0.6}As$, characterizes the periodically switched nonlinearity (PSN) [1]. For the PSN effect to occur, a medium is required in which susceptibility coefficient $\chi^{(2)}$ is modulated periodically along the direction of light propagation. We observe that in a generic case $\chi^{(2)}$ is a tensor, however most semiconductor, which crystallize in zinc-blende structures, have a symmetry and their second-order susceptibility has a single nonzero independent component (for GaAs at the transparency region below the optical energy gap $\chi_{x,y,z}^{(2)}$= 200 pm/V). The grating 1 couples the fundamental mode with the SH one. The period $\Lambda_1$=2.31*10$^{-6}$ μm satisfies the QPM condition (phase mismatch δ=0):

$$2\beta^{\omega} + \frac{2\pi}{\Lambda_1} = \beta^{2\omega} \quad \text{or} \quad \Lambda_1 = (\lambda_{FU})/(N^{2\omega} - N^{\omega}) \tag{29}$$

where $N^{\omega,2\omega}$ are the effective refractive indices of both modes. The duty ratio *a* is assumed equal to ½. In Fig. 4 we show the normalized coupling coefficient $k_{NL}$ versus *z* obtained by applying the QPM condition. Usually the input power is of the order of 1-100 mW [1], but the SH conversion requires high intensity fundamental power. For this purpose the grating 2 is designed in order to enhance the fundamental power inside the waveguide through the coupling with the scattered field generated by the fundamental mode $A^{\omega}$(z). In this case the set of equations to solve are (18) and (25) with the initial conditions $A^{\omega}(0)=(P_0)^{1/2}$ and $A^{2\omega}(0)$= 0 where $P_0$ is the input pump power. Moreover the grating 3 is added in order to optimize the SH conversion efficiency by increasing the SH coupled power. Concerning the grating 3 the set of equations to solve are (18) and (27) with the initial conditions $A^{\omega}(0)=A^{\omega}(L_1)$ and $A^{2\omega}(0)=A^{2\omega}(L_1)$. The period $\Lambda_2$ and $\Lambda_3$ satisfy the propagation condition (10) and provide a constructive interference given by the phase matching condition (15) between the incident and the scattered field. In particular we choose a strong coupling condition by analyzing the coupling coefficient versus the period and versus the *z*-direction. Figure 5 shows that regular coupling coefficients $k_S^{\omega,2\omega}$ (strong coupling) are obtained with $\Lambda_2$=0.95*10$^{-6}$ μm and $\Lambda_3$=1*10$^{-6}$ μm. The plots of Fig. 5(a) and Fig. 5(b) are obtained by evaluating the scattered fields $E_y^S$ (see Fig. 6(a) and Fig. 6(b)) generated by the fundamental and SH modes. Figures 7 and 8 illustrates the normalized substrate coupling coefficientsμ $k_S^{\omega}$ and $k_S^{2\omega}$ versus *z*-propagating direction. The SH conversion efficiency is given by $\eta(z)=|A^{2\omega}(z)|^2/|A^{\omega}(0)^2|$ [8]. Figure 9 shows the analytical solution of the conversion efficiency η by considering the grating 1, the grating 1 with the effect of the grating 2, and finally the effect of the three grating together by fixing a reference length of $L_1$=2mm. The input power used during the calculus is $P_0$ =100 mW. A conversion efficiency of about 70 % is obtained after a length of *z*=10 mm. It is clear from the Fig. 9 that the grating 3 increases the efficiency of about 20 % (optimization) respect to the case of grating 1 combined with the grating 2. In this way is possible to reduce the total length of the device by overcoming the problems of losses and reflections along the propagating direction. Concerning the total length of the structure, we observe that the theoretical effective interaction length [8] $L_{eff}\cong 2.4(\Lambda_1/2a)^{1/2}$ =3.6 mm not considers the variation of the fundamental power along the longitudinal direction, and not takes into account the grating parameters h and t which characterize the power reflected on

#106111 - $15.00 USD Received 7 Jan 2009; revised 24 Feb 2009; accepted 9 Mar 2009; published 13 Apr 2009

each step discontinuity, thus, in our practical case, a high interaction efficiency is obtained with grating lengths larger than $L_{eff}$. Moreover the choice of the parameter h=t=0.025 μm is justified by the following considerations. As reported in Fig. 10, low reflection coefficients [5] $\Gamma^{\omega,2\omega}=(\beta_d{}^{\omega,2\omega}-\beta_D{}^{\omega,2\omega})/(\beta_d{}^{\omega,2\omega}+\beta_D{}^{\omega,2\omega})$ at each step discontinuity are obtained in the single SH mode region by decreasing the values of h. But a strong coupling is obtained in the single mode SH region by increasing the h values (see Fig. 11 where are reported the coupling coefficients versus h). Figure 12 justifies the final choice of h=t=0.025 μm: the figure analyzes the numerical and analytical efficiency η versus *z* for different h values by showing a good convergence between numerical HPF, numerical two dimensional (2D) FDTD, and analytical results. A good matching between the HPF and 2D FDTD spectra is observed in Fig. 13 where we calculate the discrete Fourier transform (DFT). The convergence of the solutions confirms the accuracy of the presented theoretical model. The numerical simulations are performed by parallel calculus with time steps $\Delta t$=1.66*10-$^{16}$ sec., dimension of spatial cell $\Delta z$=0.05 μm, and sinusoidal source at $\lambda_0$= 1.55 μm given by

$$E_0^{fundamental} = \sin(\omega^{fundamental} \cdot t \cdot \Delta t) \tag{30}$$

The used numerical boundary conditions are the absorbing boundary conditions (ABCs) [13].

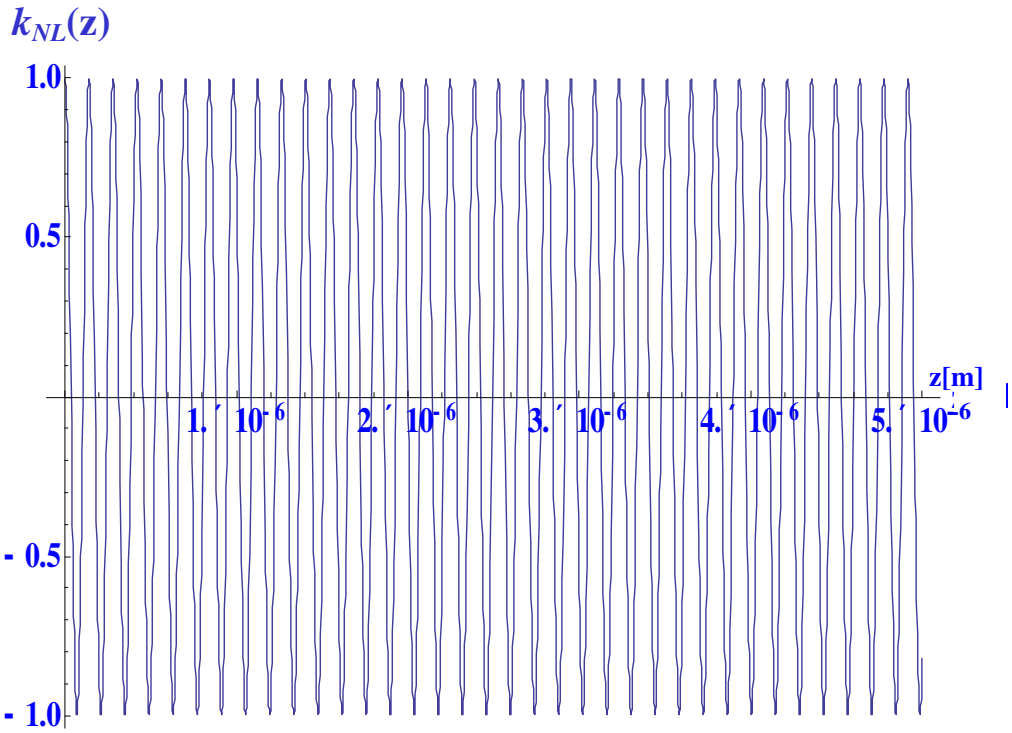


Fig. 4. Grating 1: normalized nonlinear coupling coefficient versus z.

#106111 - $15.00 USD Received 7 Jan 2009; revised 24 Feb 2009; accepted 9 Mar 2009; published 13 Apr 2009

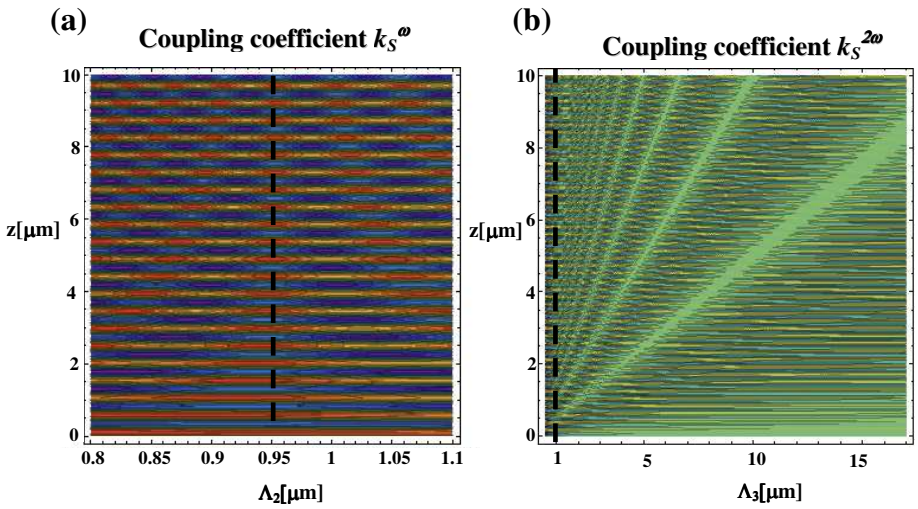


Fig. 5. Substrate coupling coefficient: (a) coupling coefficient versus $\Lambda_2$; (b) coupling coefficient versus $\Lambda_3$. Strong couplings are obtained with $\Lambda_2 = 0.95$ μm and $\Lambda_3 = 1$ μm, where the coupling coefficients are regular respect to the z- direction.

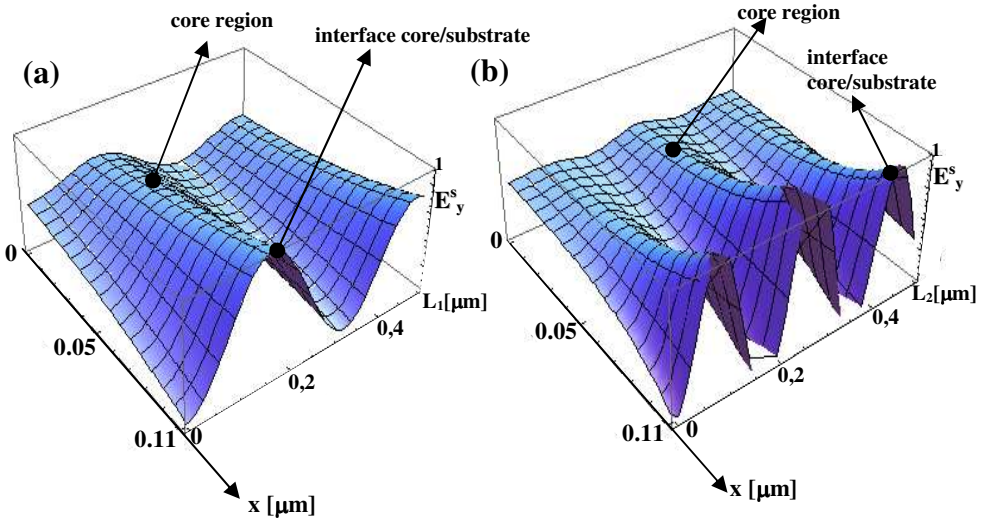


Fig. 6. (a) Scattered field generated by the fundamental mode. (b) Scattered field generated by the SH field. The coordinate system is the same of Fig. 1.

#106111 - $15.00 USD Received 7 Jan 2009; revised 24 Feb 2009; accepted 9 Mar 2009; published 13 Apr 2009

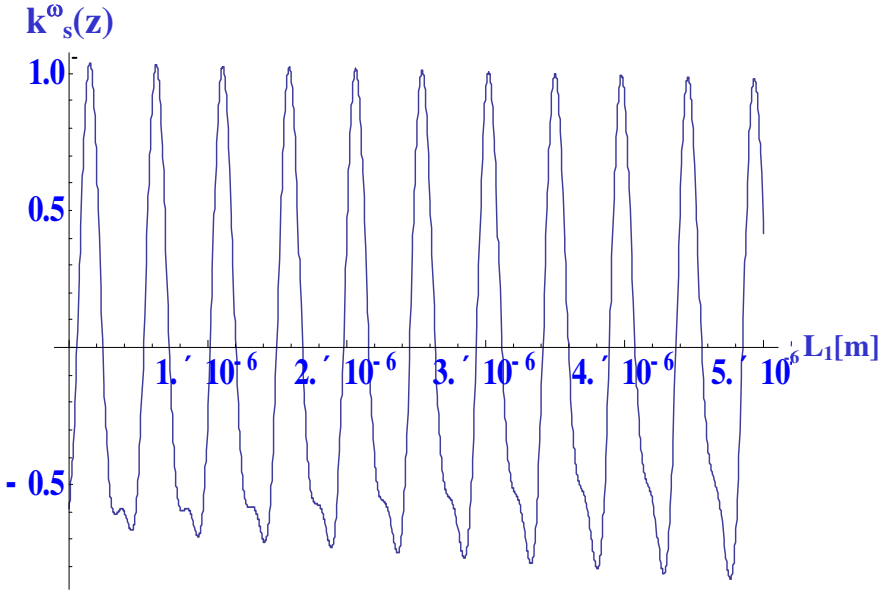


Fig. 7. Grating 2: substrate coupling coefficient versus $L_1$.

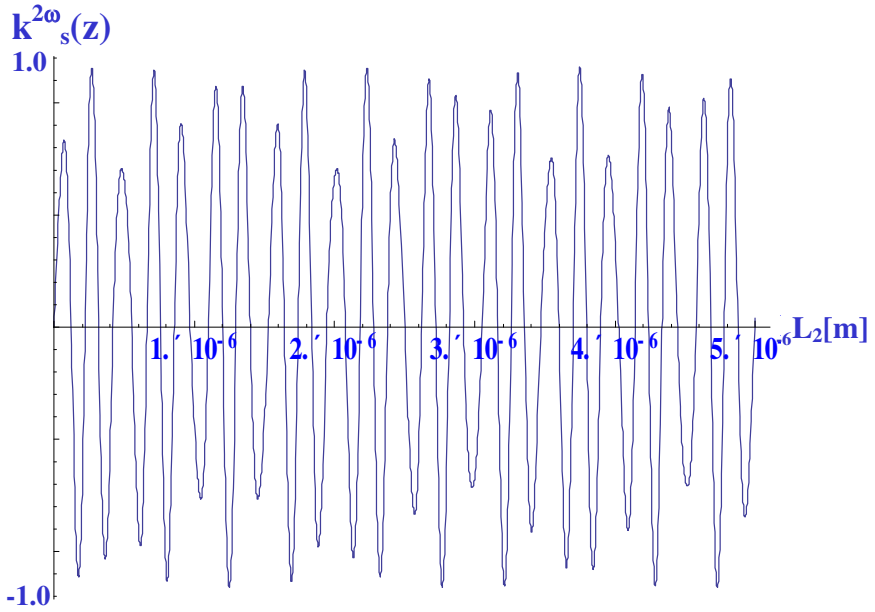


Fig. 8. Grating 3: substrate coupling coefficient versus $L_2$.

#106111 - $15.00 USD Received 7 Jan 2009; revised 24 Feb 2009; accepted 9 Mar 2009; published 13 Apr 2009

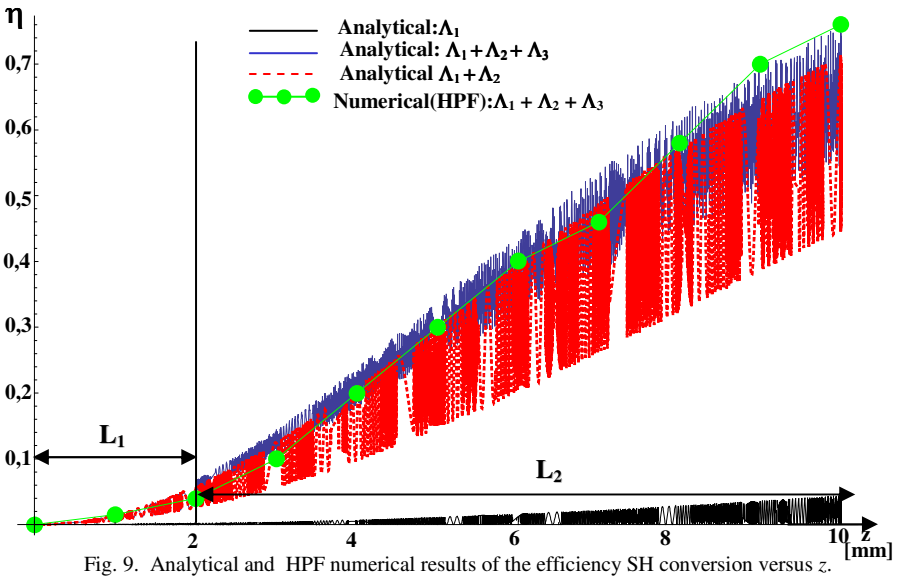


Fig. 9. Analytical and HPF numerical results of the efficiency SH conversion versus $z$.

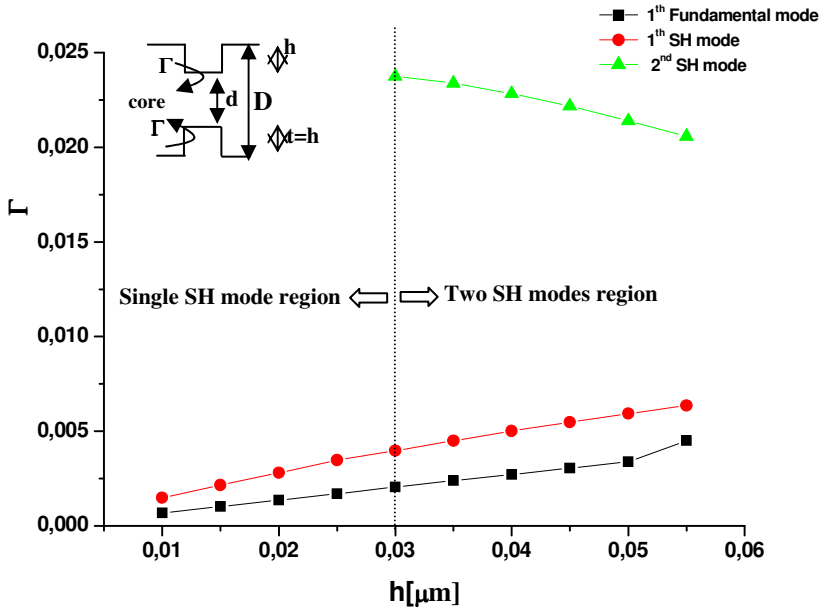


Fig. 10. Reflection coefficients $\Gamma^{\omega,2\omega}=(\beta_d{}^{\omega,2\omega}-\beta_D{}^{\omega,2\omega})/(\beta_d{}^{\omega,2\omega}+\beta_D{}^{\omega,2\omega})$ of the propagating modes at each step discontinuity. Inset: schematic diagram of a step discontinuity. The propagation constants $\beta^{\omega,2\omega}{}_d$ and $\beta^{\omega,2\omega}{}_D$ are related to region with core thickness d and D, respectively.

#106111 - $15.00 USD Received 7 Jan 2009; revised 24 Feb 2009; accepted 9 Mar 2009; published 13 Apr 2009

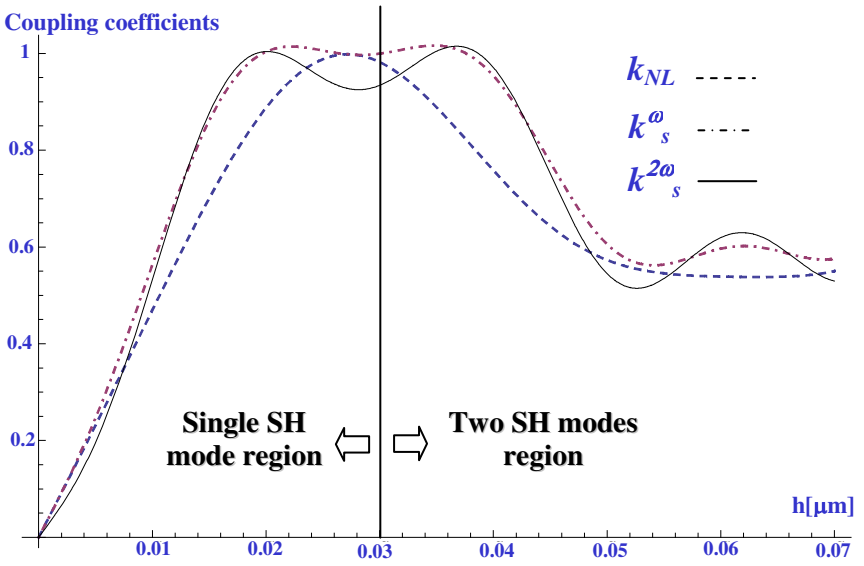


Fig. 11. Coupling coefficients versus h calculated by assuming z=0.

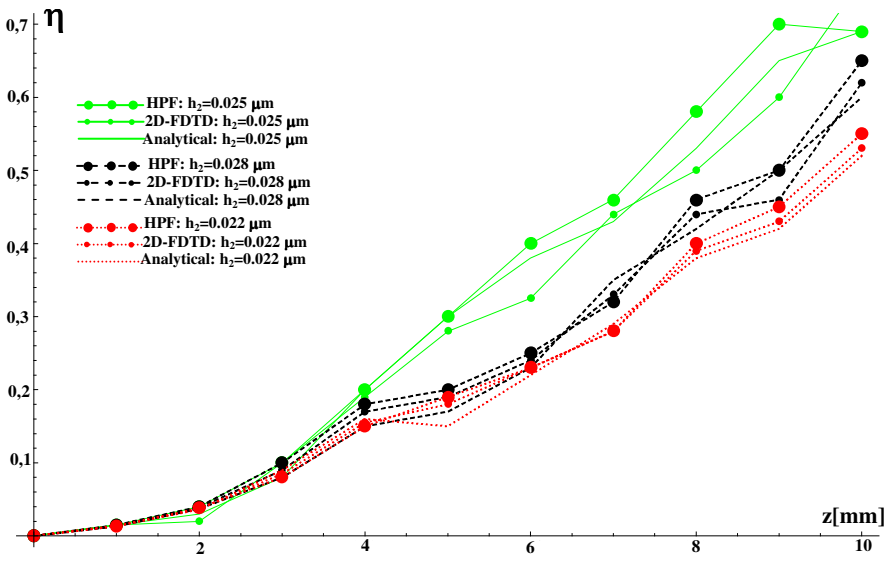


Fig. 12. Structure with grating 1, 2 and 3: analytical, 2D-FDTD and HPF results of the efficiency SH conversion versus *z* for different h values. The analytical results are averaged values.

#106111 - $15.00 USD Received 7 Jan 2009; revised 24 Feb 2009; accepted 9 Mar 2009; published 13 Apr 2009

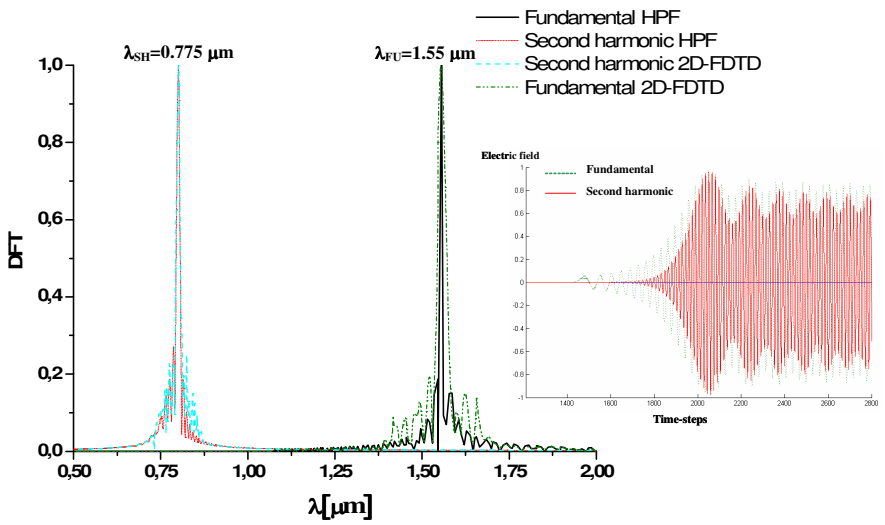


Fig. 13. Comparison between HPF and 2D-FDTD normalized spectra of the fundamental and second harmonic modes. Inset: time evolution of the fundamental and second harmonic normalized fields generated inside the waveguide of Fig. 1.

## 5. Conclusion

We presented in this work a new theoretical model for low intensity linear and nonlinear processes. The novel accurate model analyzes the effect of the radiation modes coupling on modal conversion efficiency. In particular we applied the theory in a nonlinear GaAs/AlGaAs waveguide with discontinuous core-substrate interfaces by providing design criteria for second harmonic enhancement through the use of multiple gratings. A good agreement between analytical and numerical results proves the second harmonic enhancement obtained through the radiation modes interaction. The design approach can be applied also to complex 3D optical waveguides such as ridge and channel waveguides which behave as multiplexers or polarizers. Technological and experimental works are now under study.

#106111 - $15.00 USD Received 7 Jan 2009; revised 24 Feb 2009; accepted 9 Mar 2009; published 13 Apr 2009